

**Orientation-Dependent Chemistry and Schottky-Barrier Formation at Metal-GaAs Interfaces**

S. Chang and L. J. Brillson

*Xerox Webster Research Center, Webster, New York 14580*

Y. J. Kime

*Department of Physics, Syracuse University, Syracuse, New York 13210*

D. S. Rioux

*Department of Physics, University of Wisconsin, Madison, Wisconsin 53706*

P. D. Kirchner, G. D. Pettit, and J. M. Woodall

*IBM T. J. Watson Research Center, Yorktown Heights, New York 10598*

(Received 1 February 1990)

Soft-x-ray photoemission spectroscopy of metals deposited on GaAs demonstrates that minor misorientations of the (100) surface produce major deviations from Schottky-like behavior via increased chemical interactions. The degree of chemical activity correlates with the density of dangling bonds at the [110], [111]A, and [111]B steps, producing deep levels with acceptor character which dramatically reduce the range of Fermi-level stabilization. These results demonstrate the central role of local atomic bonding in the Schottky-barrier formation.

PACS numbers: 73.30.+y

The nature of charge transfer at semiconductor interfaces has attracted considerable attention over the past five decades, driven partly by its fundamental role in solid-state processes as well as its technological applications for microelectronic devices.<sup>1,2</sup> Past efforts to understand the physical processes involved have, in general, been hampered by the insensitivity of electronic barriers to different interface conditions. However, in the past few years, researchers have obtained a much larger range of interface electronic behavior for semiconductors with a high degree of chemical and structural perfection.<sup>3</sup> Recently, we have shown that metals deposited on GaAs (100) surfaces grown by molecular-beam epitaxy (MBE) at low (90 K) temperatures under ultrahigh-vacuum (UHV) conditions exhibit near-ideal Schottky-barrier formation.<sup>4</sup> Furthermore, with increasing temperature these junctions exhibit increased chemical interaction and substantial changes in barrier height, indicating that extrinsic states form at the chemically degraded interfaces. Here we present soft-x-ray photoemission spectroscopy (SXPS) studies of metals on intentionally misoriented GaAs (100) interfaces to address the role of steps and orientation-dependent atomic bonding on the local interfacial chemistry and the macroscopic electronic barrier heights.

Intentionally misoriented (off axis) GaAs substrates are commonly used to facilitate nucleation and growth of epitaxial overlayers. However, the chemically active sites introduced may result in additional electronic features as well. Starting with oriented GaAs (100) surfaces with suppressed interfacial bonding, we observe increasing chemical reactions and decreasing ranges of Fermi-level ( $E_F$ ) stabilization energies which depend on

the orientation of vicinal steps and on the apparent density of dangling bonds. The latter density correlates closely with the density of midgap acceptor levels required to account for the altered electrostatic properties. These results reveal a pronounced effect of local atomic bonding in forming the interface chemical and electronic properties.

MBE-grown GaAs (100) layers on GaAs substrates (Sumitomo Electric) were 7500 Å thick with  $n = 5 \times 10^{16}$  cm<sup>-3</sup> doping and orientation precise to within  $\pm 0.1^\circ$ . Intentionally misoriented specimens were grown on staircaselike GaAs substrates that had been cut  $2^\circ$  off (100) toward the [110] crystal direction ((100) $2^\circ$ -[110]), toward [111] with steps consisting of Ga atoms ((100) $2^\circ$ -[111]A), and toward [111] with steps consisting of As atoms ((100) $2^\circ$ -[111]B). An As layer > 1000 Å thick deposited over the epilayers prior to removal from the growth chamber protected the surfaces from ambient contamination before thermal desorption in the analysis chamber. Thermal decapping in UHV consisted of a series of ramped anneals up to temperatures as high as 570°C. SXPS valence-band spectral features and core-level stoichiometry provided sensitive gauges of surface electronic and chemical quality, respectively,<sup>4</sup> with  $E_F$  positions derived from rigid core-level shifts and the initial  $E_F$  position above the valence-band maximum (VBM). Chamber pressures during metal evaporation were  $6 \times 10^{-10}$  Torr for Au down to  $(2-3) \times 10^{-10}$  Torr for Al. A cryotip refrigerator maintained the specimens at a thermocouple-measured temperature of 90 K during evaporation and analysis. We measured bulk (surface)-sensitive As 3d (Ga 3d) core levels using photon energies  $h\nu = 60$  and 40 eV (100 and 80 eV), respectively, in

order to monitor subsurface core-level shifts (surface chemical reactions and overlayer attenuation). Overall monochromator-electron spectrometer resolution was 0.25–0.35 eV.

Figure 1 illustrates the effect of off-axis growth orientation on the chemical reaction between GaAs and a thin, metallic overlayer. Here surface-sensitive Ga 3*d* core-level spectra for 5-Å Al on various GaAs epilayers are normalized to similar peak heights to emphasize line-shape changes and compensate for energy shifts due to band bending. Deconvoluted Ga 3*d* spectral features reveal unresolved doublets due to the substrate and, shifted to lower binding energy, dissociated Ga atoms in a metallic environment. For the oriented GaAs (100) surface (curve *a*), a 5-Å Al overlayer produces only a marginally detectable Ga dissociation, indicative of reduced chemical interaction. With increasing coverage,

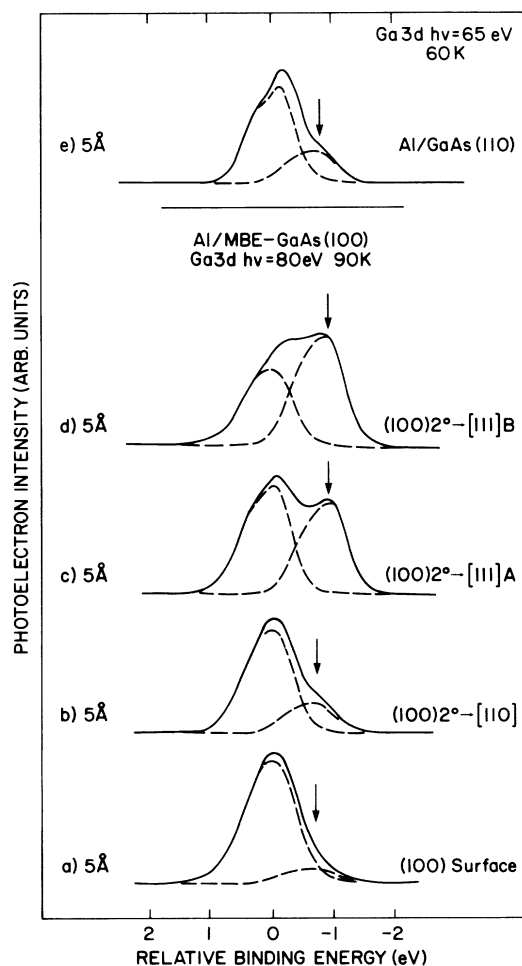


FIG. 1. Ga 3*d* core-level spectra at 5-Å deposited Al on clean surfaces for the orientations indicated. Analogous UHV-cleaved GaAs(110)/Al interface (Ref. 8) shown for comparison. Dissociated Ga peaks (indicated by arrows) reflect extent of reaction and increase with increasing density of active sites.

both Ga and As core-level intensities attenuate rapidly, consistent with uniform layer growth rather than island formation.<sup>5</sup> Associated Al 2*p* core-level spectra<sup>5</sup> show evidence of surface<sup>6</sup> rather than subsurface<sup>7</sup> bonding. For Al on GaAs(100)2°-[100] (curve *b*), evidence of Ga dissociation is clearly visible and is comparable to that reported by Aldao<sup>8</sup> for UHV-cleaved GaAs(110)/Al interfaces at a lower temperature and similar surface-sensitive energy (curve *e*). Here the Al 2*p* spectra reflect more extensive interface bonding.<sup>5</sup> The relative intensity of the dissociated Ga feature continues to increase with (100)2°-[111]*A* (curve *c*) and finally (100)2°-[111]*B* orientation (curve *d*), dominating the substrate feature in the latter. As with previous Al studies for GaAs, As 3*d* line shapes for these MBE-grown surfaces exhibit virtually no observable line-shape changes. With increasing overlayer thickness, Ga attenuation slows and dissociation increases in the same order as Fig. 1. In contrast, As core-level intensities continue to attenuate rapidly for all orientations, ruling out significant effects due to morphology as opposed to atomic structure.

SXPS measurements of analogous Au/GaAs experiments also display an increase in outdiffusion in the order (100), (100)2°-[110], (100)2°-[111]*A*, and (100)2°-[111]*B* with both Ga and As outdiffusion evident but with only minor line-shape changes.

Figure 2 illustrates the  $E_F$  movement within the GaAs band gap as a function of metal coverage for both Al and Au on the four surfaces discussed in Fig. 1.  $E_F$  positions for the clean surfaces are 0.2–0.3 eV below the conduction-band minimum (CBM). As with previous low-temperature work,<sup>9</sup> little or no *n*-type band bending is observable up to 1 Å for all systems. This photovoltaic effect<sup>10</sup> is eliminated by metallization at the highest coverages illustrated.<sup>11</sup> For the oriented GaAs(100) sur-

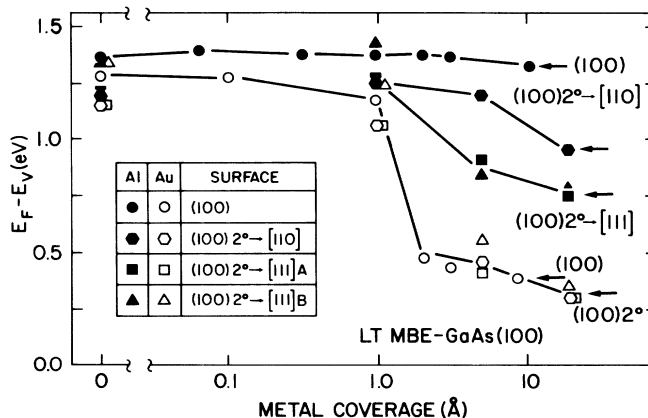


FIG. 2. Fermi-level movements within the GaAs band gap as a function of Au or Al deposition for the same (100)-oriented and -misoriented surfaces as Fig. 1. Al band bending varies by > 0.5 eV for different orientations, whereas Au band bending is relatively unaffected.

face, 10-Å Au deposition produces large band bending with  $E_F - E_{VBM} = 0.35$  eV (open circles), whereas 10-Å Al coverage has little or no effect,  $E_F - E_{VBM} = 1.25$ –1.3 eV (solid circles). For Au on misoriented surfaces (open hexagon =  $(100)2^\circ$ -[110], open square =  $(100)2^\circ$ -[111]A, open triangle =  $(100)2^\circ$ -[111]B),  $E_F$  movement with increasing thickness differs only slightly from the (100) surface. In contrast, Al on misoriented GaAs(100) produces significant changes in band bending with respect to oriented surfaces. For Al on GaAs(100) $2^\circ$ -[110] (filled hexagons),  $E_F$  moves down to 0.95 eV above  $E_{VBM}$  at 12 Å. For Al on GaAs(100) $2^\circ$ -[111]A (open squares) and (100) $2^\circ$ -[111]B (open triangle) surfaces,  $E_F$  moves down to midgap, 0.75–0.77 eV above  $E_{VBM}$ . As a result, the range of  $E_F$  movement between Au and Al decreases from 0.92 eV for the oriented (100) surface, to 0.65 eV for the (100) $2^\circ$ -[110] face, to 0.46 eV or less for the (100) $2^\circ$ -[111] surface. Hence, Fig. 2 demonstrates that relatively small misorientations of the GaAs(100) substrate (with the same line density of defects) can result in major electronic effects.

The orientation dependence of Al/GaAs Schottky-barrier height requires corresponding differences in the density of charge localized at the interface. Figure 3 illustrates results of a self-consistent electrostatic calculation<sup>12</sup> to account for the Au and Al barrier-height dependence on work function reported here in terms of

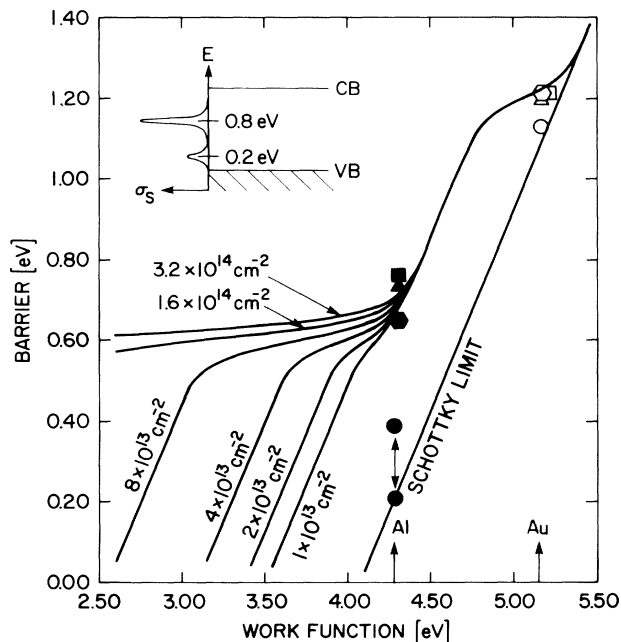


FIG. 3. Self-consistent electrostatic analysis of the metal/GaAs (100) data points. The family of curves represent acceptor densities of  $3 \times 10^{13} \text{ cm}^{-2}$  at  $E_{VBM} + 0.2$  eV and indicated densities at  $E_{VBM} + 0.8$  eV (see inset). Deviations from the Schottky line correspond to midgap densities which scale with active site densities for the various orientations.

equivalent deep level energies and densities. Theoretically the deviations from ideal Schottky behavior (Schottky-limit line) require two acceptor states located 0.2 and 0.8 eV above  $E_{VBM}$ . States at these energies with different 0.8-eV state densities and a 0.2-eV density of  $3 \times 10^{13} \text{ cm}^{-2}$  describe in detail the barrier-height versus work-function dependence for a wide variety of metals on room-temperature GaAs(100).<sup>13</sup> Furthermore, cathodoluminescence spectra have yielded direct evidence for states at these energies.<sup>14</sup> For the oriented GaAs(100), the Au and Al data (as well as other metals<sup>15</sup>) lie near or on the Schottky-limit line. The double-headed arrow indicates the range of barrier heights observed in several oriented (100) experiments using SXPS and internal photoemission spectroscopy. For the oriented GaAs(100) at 90 K, metal barrier heights are consistent with acceptor densities well below  $10^{13} \text{ cm}^{-2}$ . The increase in Al/GaAs(100) barrier height with misorientation requires an increase in 0.8-eV acceptor density. Previously we have demonstrated the sensitivity of this state to interface chemical reaction.<sup>14</sup> For the (100) $2^\circ$ -[110] surface, the barrier shift to 0.55 eV requires a minimum of  $1 \times 10^{13} \text{ cm}^{-2}$  states. Likewise, a density of  $(5-10) \times 10^{13} \text{ cm}^{-2}$  accounts for the shift to 0.75/0.77 eV for the (100) $2^\circ$ -[111] surfaces. These densities correlate with the active site densities for different step orientations. Although the reconstruction(s) of the vicinal surfaces (along with preparation-dependent double steps and facets) are not yet established, the unreconstructed surfaces highlight the difference in atomic density and the nature of the associated dangling bonds for the different misorientations. For a  $2^\circ$  misorientation, line density of steps with a height  $a_0/2 = 2.828 \text{ \AA}$  is  $1.234 \times 10^6 \text{ cm}^{-1}$ . For unreconstructed step faces, atom spacing parallel to the step edge is  $a_0$  for (110) and  $a_0/\sqrt{2}$  for (111). Hence the density of either As or Ga edge sites is  $2.18 \times 10^{13} \text{ cm}^{-2}$  for (100) $2^\circ$ -[110] surfaces and  $3.09 \times 10^{13} \text{ cm}^{-2}$  for (100) $2^\circ$ -[111] surfaces. The [110] densities account rather well for the 0.4-eV Al barrier increase shown in Fig. 3. The additional densities of states for [111] steps contributes to the additional barrier increase of 0.1–0.15 eV, although a 2–5 times higher density is suggested by the fit.

The relatively small changes in Au/GaAs barrier heights are consistent with the formation of the 0.2-eV acceptor states with comparable densities. Barriers for such high work-function metals are unaffected by changes in midgap acceptor density. Furthermore, either the midgap levels must have only acceptor character or, if they have donor character, Au deposition must produce them only inefficiently.

The reaction products illustrated in Fig. 1 suggest proportionally larger densities of chemically active sites for the (111) vs (110) step face. Relative to the unreacted surface Ga 3d signals, the dissociated peak intensities in

Fig. 1 increase as 15:30:85:144. The proportionally larger extent of (111) interface reactions versus edge sites suggest the creation of additional electrically active sites. In fact, differences in chemical activity provide a link between electrically active site density and local atomic bonding. Gatos, Moody, and Lavine<sup>16</sup> showed that group-V-terminated surfaces are much more chemically active than their group-III counterparts because of the former's unshared pair of electrons. Consistent with this higher surface As activity, they reported relative rates of reactivity based on chemical etching and oxidation in the order  $[111]B > [111]A \approx [100] > [110]$ . For the thermally treated (100) surfaces used here,<sup>4</sup> the (measured) As surface deficiency should decrease in reactivity further. In addition, the Al epitaxy to GaAs(100) may well retard chemical interaction. Thus the relative differences in reactivity in Fig. 1 appear to follow straightforward chemical arguments.

The high stability of the oriented GaAs (100) surface is consistent with a metal-insulator-semiconductor picture of metal/GaAs (100) Schottky-barrier formation recently proposed by Freeouf *et al.*<sup>17</sup> Energy-minimization calculations of Larsen and Chadi<sup>18</sup> suggest that the most stable (100) reconstruction of GaAs involves a large ordered surface fraction of As vacancies, dimer ordering of the remaining surface atoms, and a significantly larger band gap. Such an insulating surface layer should attenuate effects of any metal-induced gap states on the  $E_F$  stabilization. The high sensitivity of Al barrier heights to local atomic bonding also accounts for their considerable variability in previous studies.<sup>13</sup>

In conclusion, our results demonstrate that minor misorientations of the GaAs (100) surface can produce major deviations from Schottky-like behavior via increased chemical interactions. Step orientation rather than the presence of steps alone determines densities of chemically active sites at step edges, which in turn results in order-of-magnitude changes in reaction and diffusion. The resultant electrical junctions exhibit dramatically different Schottky-barrier formation and interface state densities which correlate with the differences in microscopic chemical bonding.

The authors wish to acknowledge valuable conversations with D. J. Chadi and R. E. Viturro and support in part by the U.S. Office of Naval Research through Contract No. N00014-80-C-0778 and by the National Science Foundation, which supports the Synchrotron Radiation Center of the University of Wisconsin-Madison.

<sup>1</sup>L. J. Brillson, Surf. Sci. Rep. **2**, 123 (1982).

<sup>2</sup>E. H. Roderick and R. H. Williams, *Metal-Semiconductor Contacts* (Clarendon, Oxford, 1988), 2nd ed.

<sup>3</sup>L. J. Brillson, Comments Condens. Matter Phys. **14**, 311 (1989).

<sup>4</sup>R. E. Viturro, J. L. Shaw, C. Mailhot, L. J. Brillson, N. Tache, J. McKinley, G. Margaritondo, J. M. Woodall, P. D. Kirchner, G. D. Pettit, and S. L. Wright, Appl. Phys. Lett. **52**, 2052 (1988).

<sup>5</sup>S. Chang *et al.* (unpublished).

<sup>6</sup>R. Z. Bachrach, J. Vac. Sci. Technol. **15**, 1340 (1978).

<sup>7</sup>A. Kahn, L. J. Brillson, G. Margaritondo, and A. D. Katanani, Solid State Commun. **38**, 1269 (1981).

<sup>8</sup>C. M. Aldao (private communication).

<sup>9</sup>For example, K. Stiles and A. Kahn, Phys. Rev. Lett. **60**, 440 (1988).

<sup>10</sup>M. H. Hecht, Phys. Rev. B **41**, 7918 (1990); J. Vac. Sci. Technol. B (to be published).

<sup>11</sup>S. Chang, I. Vitomirov, L. J. Brillson, D. Rioux, P. D. Kirchner, J. M. Woodall, and M. L. Hecht (unpublished).

<sup>12</sup>C. B. Duke and C. Mailhot, J. Vac. Sci. Technol. B **3**, 1170 (1985).

<sup>13</sup>L. J. Brillson, R. E. Viturro, J. L. Shaw, C. Mailhot, N. Tache, J. McKinley, G. Margaritondo, J. M. Woodall, P. D. Kirchner, G. D. Pettit, and S. L. Wright, J. Vac. Sci. Technol. B **6**, 1263 (1988).

<sup>14</sup>R. E. Viturro, J. L. Shaw, and L. J. Brillson, J. Vac. Sci. Technol. B **6**, 1397 (1988).

<sup>15</sup>R. E. Viturro, S. Chang, J. L. Shaw, C. Mailhot, L. J. Brillson, R. Zanon, Y. Hwu, G. Margaritondo, P. D. Kirchner, and J. M. Woodall, J. Vac. Sci. Technol. B **7**, 1007 (1989).

<sup>16</sup>H. C. Gatos, P. L. Moody, and M. C. Lavine, J. Appl. Phys. **31**, 212 (1960).

<sup>17</sup>J. L. Freeouf, J. M. Woodall, L. J. Brillson, and R. E. Viturro, Appl. Phys. Lett. **56**, 69 (1990).

<sup>18</sup>P. K. Larsen and D. J. Chadi, Phys. Rev. B **37**, 8282 (1988); (private communication).